Revista Mexicana de Astronomía y Astrofísica, **43**, 257–270 (2007)

FORMATION OF A TWO-DENSE-RINGS-PATTERN DISK FROM THE COLLAPSE OF A CLOUD

E. Nagel

Instituto de Astronomía
Universidad Nacional Autónoma de México

Received 2006 November 28; accepted 2007 March 02

RESUMEN

En este artículo se estudia la formación de un disco, que resulta del colapso de una nube rotando rígidamente. El plano perpendicular al eje de la velocidad angular que contiene a la estrella es la superficie donde el material que cae de ambos lados se encuentra, formando así una estructura de choque de dos capas. El material chocado se mueve casi paralelo a este plano, siendo éste el material que forma el disco. Desarrollamos una simulación axi-simétrica e isoterma usando como condición inicial una aproximación balística para las trajectorias de las partículas localizadas en la vecindad de la estrella. La evolución dinámica de este material, incluyendo el material que continuamente se incorpora de la nube, lleva al disco a una configuración estacionaria que consta de dos anillos densos de momento angular específico constante que se encuentran en una posición kepleriana. Un rasgo como éste puede cambiar el espectro de estos discos en etapas muy embebidas.

ABSTRACT

In this paper, the formation of a disk resulting from the collapse of a rigidly-rotating cloud is studied. The plane perpendicular to the angular velocity axis that contains the star is the locus where materials falling from both sides face each other with the consequent formation of a double layer shock structure. The shocked material that moves almost parallel to this plane is the material that forms the disk. A hydrodynamical axisymmetric and isothermal simulation is developed using as initial condition a ballistic approximation for the trajectories of the particles located in the vicinity of the star. The dynamical evolution of this material, including the material that is continuously incorporated from the cloud, drives the disk to a stationary configuration composed of two dense rings with constant specific angular momentum that sit on Keplerian positions. A feature like this can change the spectra of disks in deeply embedded stages.

Key Words: **ACCRETION, ACCRETION DISKS — CIRCUMSTELLAR MATTER — HYDRODYNAMICS — STARS: FORMATION**

1. INTRODUCTION

One of the main topics in interstellar studies is the formation of a star from material of a molecular cloud. Another result of this process is the formation of a rotating disk around the stellar system. This part of the phenomenon is a natural outcome of the collapse of a cloud with angular momentum (Shu, Adams, & Lizano 1987). Observationally, the presence of a disk is by now accepted for many objects (Padgett, Stapelfeldt, & Sargent 2000; Hayashi, Ohashi, & Miyama 1993; Strom, Edwards, & Skrutskie 1993; Mundy, Looney, & Welch 2000), owing to the information of infrared and millimeter wavelengths that trace dust or molecular gas in the vicinity of the star. The natural state of the disk is that in which its material is moving in circular orbits around the star with Keplerian velocity, slowly accreting towards the star via viscosity dissipation (Lynden-Bell & Pringle 1974), working on a slower time scale than the free-fall time of the collapse of the cloud (Tscharnuter & Boss 1993) to form the star-disk system.

The lack of information on the early stages of disk formation is surmounted with collapse calculations using numerical codes (Larson 1972; Hueso & Guillot 2002, 2005; Tscharnuter & Boss 1993; Shu et al. 1987) or with the semi-analytic description of the infall from a cloud with angular momentum (Terebey, Shu, & Cassen 1984). The description of the formation of a disk requires a solution that is valid near the star which asymptotically joins the similarity solution given in Terebey et al. (1984). A disk will form from the collapse of a cloud with some rotation, a problem which was solved by Terebey et al. (1984). They solve the collapse in an intermediate zone between a marginally stable configuration far from the star and the innermost part of the cloud where rotation becomes essential for describing the kinematics. The inner solution was developed by Ulrich (1976) and Cassen & Moosman (1981) and due to supersonic velocities, pressure effects can be neglected so that two-body solutions (Cassen & Moosman 1981; Ulrich 1976) correctly represent the trajectories of the particles that are falling from a rigidly rotating cloud. This solution for material that falls into a disk was used by Lin & Pringle (1990) and recommended in Stahler et al. (1994) as a natural initial condition for simulations addressing the problem of disk formation and evolution. The main assumption required to use the solution described in Ulrich (1976) is that the mass of the star rules over the mass in a disk, or over the material in the falling envelope; besides it is not relevant in which stage of the evolution the system is. An essential difficulty in numerical studies of the collapse of a cloud is that the range in density spans several orders of magnitude (Bate 2000), and if one also wants to study the dynamical details of the evolution in the inner part of the cloud on small time-scales, the problem demands a titanic effort. Thus, some kind of approximation is always required, such as using the density and velocity field in Ulrich (1976). However, the arguments and papers referred to above are enough to allow these expressions to be taken as initial conditions in the hydrodynamical simulation described in § 4.

In this paper we are interested in the formation and early evolution of a disk. Formation means the stage where material falls from the cloud to the plane perpendicular to the angular momentum vector which contains the star, and early evolution means the description of the motion of the material that arrives to this plane at some time and moves parallel to it. As long as we have a thin proto-disk, at least an order of magnitude less massive than the star, and material is still falling from the cloud, then at this particular time, early evolution can be described. The angular velocity axis defines a symmetry plane called orbital plane, which is perpendicular to this axis and contains the star. Thus, a collapse of a cloud naturally produces shocks almost parallel to this plane (Yorke & Bodenheimer 1999; Laughlin & Bodenheimer 1994; Cassen & Moosman 1981; Bodenheimer & Laughlin 1995), above and below the disk that is forming.

In previous works a detailed study of this stage is missing (Nakamoto & Nakagawa 1994; Lin & Pringle 1990; Cassen & Moosman 1981), because of the demand that the material falling from the cloud to the disk would quickly dissipate energy and the radial component of its velocity would smoothly incorporate to a Keplerian disk with the help of strong turbulent interactions in the post-shock region. The energy resulting from dissipation of the velocity component perpendicular to the orbital plane has an easy explanation using a symmetry argument; however, the vanishing radial velocity is a fact that one can expect, because circular orbits are the obvious configuration, but requires a more detailed study, like the one carried out here. Stahler et al. (1994) tell us more about this early stage by solving the inviscid and pressure-free fluid equations on the orbital plane with a term that represents the contribution from the material that falls from the cloud with the solution given by Cassen & Moosman (1981). Using typical quantities, the partial time derivatives can be neglected, ending up with a steady state solution as a good approximation. This estimation allows us to describe the system as quasi-statically evolving from one steady state to another, where the mass of the star continuously increases. In the same way, in Nagel (2007) a similar argument is presented to argue that the pattern in the disk can survive a certain time until eventually it is destroyed by gravitational instabilities. Interesting enough is the formation of a dense ring, a feature always present in the disk description of Stahler et al. (1994), and also in our hydrodynamical simulation.

The existence of dense structures inside a disk is relevant to the study of the formation of planets or companion stars. Many cloud collapse simulations (Tohline 1980; Pickett, Mejía, & Durisen 2003; Boss 1980; Larson 1972; Black & Bodenheimer 1976; Bodenheimer & Tscharnuter 1979) have as an outcome the formation of rings. The idea behind this process (for details see Tohline 1980) is that certain configurations allow the existence of a zone where positive forces (centrifugal, pressure...) can compete

with net gravitational forces, which in a collapse situation always point in the negative direction, towards the center of mass.

At a certain location inside this region, positive and negative forces cancel each other. During some span of time, after the fulfillment of the last situation, some material moves in the opposite direction, sweeping particles on its way out and getting denser, to become a well-defined structure.

Gravitational instabilities are recognized as a major cause of outward transport of angular momentum with the corresponding accretion of mass towards the star. Also Shu, Najita, & Ostriker (1994) speculate that these instabilities self-regulate the amount of mass in the disk during the stage of infall of material from the cloud to the disk. In other words, massive disks easily develop instabilities that transport mass to the star until the disk is well below a threshold mass. This kind of instability is observed in numerical simulations (Bodenheimer & Laughlin 1995; Yorke & Bodenheimer 1999; Nakamoto & Nakagawa 1994; Boss 1998) of a rotating disk and is studied analytically in Hunter (1963), clearly identifying an infinite number of axisymmetric and non-axisymmetric modes in which a disk is unstable. Of course, the details depend on the density and angular velocity profile along the disk. Any of these instabilities could be responsible for the destruction of axisymmetric structures like rings; its relevance to the problem at hand is beyond the scope of this paper.

The aim of this paper is to fill a part of the gap existing in the study of the very early stage of disk formation. Most of the time, the disk exists in a state of non-accretion from the cloud (Shu et al. 1994), so observations will commonly show an evolved disk, established in a Keplerian configuration, such as that Mundy et al. (2000) use to describe their observations. However, in this paper we want to stress that it is natural to think of other stationary disk configurations to compare with observations. It is difficult to think that these dense features can be found in non-embedded sources, where the disk has had enough time to evolve; however, Piétu, Guilloteau, & Dutrey (2005) observed the surroundings of AB Auriga, and found non-Keplerian motion that they say could be produced in an early stage of star formation. A centrally peaked spiral-like feature appears, which cannot be explained in a traditional Keplerian T Tauri disk, so the work of Piétu et al. (2005) found a fine example of a system that apparently requires mechanisms in previous stages which can form dense structures. We do not intend to impose any kind of assumption on the final configuration of the disk, but allow it to find its way to a stationary configuration. The basic idea of this work is to initially impose the density and velocity field given in Ulrich (1976) on the collapsing envelope around the star, allowing a shock in the orbital plane to naturally form a disk, and to follow this system until it comes to a stationary state.

This paper is organized as follows. § 2 gives a detailed explanation of the problem at hand and of all the ingredients its solution requires. § 3 gives an analytic solution which allows us to describe the evolution of a non-interacting ring of material in the disk, as a function of angular momentum. The main result is presented in § 4, where we describe an axisymmetric 2D hydrodynamical simulation, using as initial condition the density and velocity field given in Ulrich (1976). Nagel (2007) gives a detailed explanation of the arguments in favor of the viability of this specific configuration using the fact that the stationary configuration is reached in a relatively short time as compared with the lifetime of the infall stage. Nagel (2007) presents the results of a Lagrangian simulation, that, with several assumptions, addresses the dynamic problem in the orbital plane, in a quest to understand the involved physics by means of a simple model. § 5 is a summary of our study, while the conclusions are given in § 6.

2. GENERAL DESCRIPTION OF THE PROBLEM

The two parts into which we divide the system are the central star and the material that is falling in due to the gravitational potential of the star. The interactions between these parts are manifold, but the one considered here is only the gravitational force between an individual particle and the central mass. A strong assumption is that the gravity between the particles of the cloud around the star is weak as compared to the interaction with the star itself. This is true because in the inner portion of the cloud self-gravity can be neglected (Terebey et al. 1984) and ballistic trajectories (Cassen & Mossman 1981) can be used as an initial conditions in a simulation.

We study the first stages of formation of a disk, when material from the cloud is just arriving at the vicinity of the star. The principal condition for a disk to be formed is that the particles that fall in shall have some angular momentum; otherwise, they move directly into the central mass with no chance for a disk to exist, or even to form.

The simplest assumption for the infalling cloud is that it is rigidly rotating; it is the one we use here.

A model with all these hypotheses was developed in Ulrich (1976) where the particle begins at infinity with null radial velocity and a total velocity that is very low compared with the velocity acquired at the time when it is reaching the vicinity of the star. Thus, a good approximation is to set a null energy to every particle (so, the trajectories are parabolas), which is conserved in a central potential, as well as a specific angular momentum. Ulrich (1976) found the following velocity field,

$$v_r = -\left(\frac{1}{r}\right)^{\frac{1}{2}}\left(1+\frac{\cos\theta}{\cos\theta_{\rm o}}\right)^{\frac{1}{2}}, \quad (1)$$

$$v_\theta = \left(\frac{1}{r}\right)^{\frac{1}{2}}\frac{\cos\theta_{\rm o}-\cos\theta}{\sin\theta}\left(1+\frac{\cos\theta}{\cos\theta_{\rm o}}\right)^{\frac{1}{2}}, \quad (2)$$

$$v_\phi = \left(\frac{1}{r}\right)^{\frac{1}{2}}\left(1-\frac{\cos\theta}{\cos\theta_{\rm o}}\right)^{\frac{1}{2}}\frac{\sin\theta_{\rm o}}{\sin\theta}, \quad (3)$$

and the orbit is described by the equation

$$r = \frac{\sin^2\theta_{\rm o}}{(1-\frac{\cos\theta}{\cos\theta_{\rm o}})}, \quad (4)$$

and, finally, the density is given by,

$$\rho = r^{-\frac{3}{2}}\left(1+\frac{\cos\theta}{\cos\theta_{\rm o}}\right)^{-\frac{1}{2}}\left(1+\frac{3\cos^2\theta_{\rm o}-1}{r}\right)^{-1}, \quad (5)$$

where (r,θ,ϕ) are the spherical coordinates of a particular point in space, and $\theta_{\rm o}$ is the angle with respect to the rotational axis of the cloud that defines the plane containing the trajectory of the particle.

The velocity, radius and density are given in units of:

$$v_{\rm o} = (\frac{GM}{R_{\rm d}})^{\frac{1}{2}}, \quad R_{\rm d} = \frac{\Gamma_\infty^2}{GM}, \quad \rho_{\rm o} = \frac{\dot{M}}{4\pi R_{\rm d}^2 v_{\rm o}}, \quad (6)$$

respectively, where $R_{\rm d}$ is the Keplerian radius for a particle with specific angular momentum Γ_∞, the maximum value in a spherical shell of the cloud. For the case of rigid rotation, the maximum occurs at the equator; this plane also defines the orbital plane, the locus where the disk is formed. These definitions allow us to interpret $v_{\rm o}$ as the Keplerian velocity at radius $R_{\rm d}$; this radius naturally represents the typical radius of the disk. In Equation (6), $\dot{M}$ is the mass accretion rate from the cloud, so $\rho_{\rm o}$ represents the density of the material from a spherical shell of radius $R_{\rm d}$, moving with velocity $v_{\rm o}$.

If $v_{\rm o}$ is the characteristic velocity, calculated with $R_{\rm d} = 100$ AU and $M = 1\,M_\odot$, and if the velocity of sound is calculated with $T = 15\,{\rm K}$ as the temperature of the cloud, we can conclude that the latter is an order of magnitude smaller than the former, so the flow can be considered as supersonic. Hence, the pressure gradients can be neglected and therefore a two-body model for the flow is a good approximation.

The orbital plane divides the space into two parts, each being a "mirror image" of the other. The solution of Ulrich (1976) gives two different velocities for each point in the plane, with perpendicular components having the same magnitude but in opposite directions. When the particles associated with the two velocities face each other, their velocities perpendicular to the plane are lost in an inelastic collision. In other words, two shocks are formed parallel to the plane, forcing the velocity of the shocked material to lie on that plane. Particles that are incorporated in such a way will remain there and will belong to the disk that is forming.

Using Equation (4) we can show that the orbits intersect the orbital plane ($\theta = \pi/2$) at a radius $R_{\rm I}$ given by,

$$R_{\rm I} = \sin^2\theta_{\rm o}\ . \quad (7)$$

This relation shows that the typical size of the disk ($R_{\rm d}$) is the maximum of $R_{\rm I}$. From this we can conclude that the largest radius where the shock is present is also the maximum position of a stable orbit, where stable has here the meaning of a Keplerian orbit, the locus where the centrifugal force plus the gravitational one give zero.

3. ANALYTICAL SOLUTIONS

Here, we describe the orbits in the orbital plane, taking the velocity field given in Ulrich (1976) but restricted to this plane. These velocities clearly represent the evolution in the orbital plane as long as they remain supersonic. First of all, we substitute the radius in Equation (7) in the set of Equations (1) and (3) to obtain,

$$v_{R_{\rm o}} = -\left(\frac{1}{R_I}\right)^{\frac{1}{2}}, \quad v_{\phi_{\rm o}} = 1\ , \quad (8)$$

where we have also substituted $\theta = \pi/2$.

Since the particle has lost the energy associated with its velocity perpendicular to the disk, it now has a negative total energy, which means that the resulting orbits are ellipses. The energy of the shocked particles is given by:

$$\epsilon_{\rm o} = \frac{1}{2}(v_{R_{\rm o}}^2 + v_{\phi_{\rm o}}^2) - \frac{1}{R_{\rm I}}\ . \quad (9)$$

Using Equation (8) in Equation (9) and expressing the result in terms of the specific angular mo-

mentum γ, defined by $\gamma = R_{\rm I} v_{\phi_{\rm o}}$, we have

$$\epsilon_{\rm o} = -\frac{1}{2}\frac{(1-\gamma)}{\gamma} \, . \tag{10}$$

We can now calculate the radial velocity of a particle characterized by γ and located at radius R by using conservation of energy and angular momentum. The energy per unit mass is given by

$$\epsilon_{\rm o} = \frac{1}{2}(v_R^2 + v_\phi^2) - \frac{1}{R} \, , \tag{11}$$

and the next equation is just a definition,

$$\gamma = R v_\phi \, . \tag{12}$$

Substituting Equation (12) in Equation (11) and solving for the radial velocity v_R, we obtain,

$$v_R = \pm \left[2(\epsilon_{\rm o} + \frac{1}{R}) - \frac{\gamma^2}{R^2} \right]^{\frac{1}{2}} \, . \tag{13}$$

As we mentioned before, the orbits in the orbital plane are closed; then we can calculate the minimum and the maximum distance to the star. The minimum and maximum distances are defined as the point where $v_R = 0$, and using Equations (13) and (10) we get

$$R_{\rm min,max} = \frac{\gamma(1 \pm \sqrt{1-\gamma+\gamma^2})}{1-\gamma} \, . \tag{14}$$

Notice in Equation (13) that the solution of v_R has both signs (+ or −), representing either the section of the orbit towards the star or the one in the opposite direction. We see in Equation (8) that the radial velocity is negative, indicating that the first part of the trajectory is approaching the star, and ending when the particles reach the minimum radius ($R_{\rm min}$).

Without interactions the particles will get there and start to move in the opposite direction. The description of the approaching stage begins with the solution of the equation given by

$$\frac{{\rm d}R}{{\rm d}t} = v_R \, , \tag{15}$$

where v_R is given by Equation (13). Because v_R is not a function of time, we transform the differential equation into the following integral,

$$t = \int v_R^{-1} {\rm d}R \, , \tag{16}$$

whose solution can be expressed as

$$\begin{aligned} t &= \pm \frac{1}{(-2\epsilon_{\rm o})^{1/2}} [-(R-R_{\rm min})^{1/2}(R_{\rm max}-R)^{1/2} \\ &- \frac{1}{2}(R_{\rm min}+R_{\rm max}) \\ &\quad {\rm atan}\left(\frac{(R_{\rm min}+R_{\rm max})-2R}{2(R-R_{\rm min})^{1/2}(R_{\rm max}-R)^{1/2}}\right)] \, . \end{aligned} \tag{17}$$

From the practical point of view, the difference in the evaluation of t (Equation 17) for any two points tells us, for material with angular momentum γ, the time that a specific particle needs to travel the distance between these points. In other words, we know the time of arrival of any ring of material at any position in the orbital plane. In the remaining part of this section, the word "ring" refers to a thin circular section of the disk. Due to the cylindrical symmetry of the problem, the particles contained in a ring evolve exactly in the same way.

The main drawback is that only the description of the evolution of an isolated ring, labeled with the angular momentum (conserved quantity), is obtained. If there are processes that change this value, the description becomes more complicated. In a hydrodynamical simulation, a ring is always subjected to artificial or explicit viscosity, so the assumption of conservation of angular momentum has to be somewhat relaxed.

For Equation (17) to be of any practical use the essential condition to satisfy is that the original rings evolve long enough without interactions between them. If we use Equation (17) to calculate the time for the initial rings to get to $R_{\rm min}$, we see that the time increases with γ. Because $R_{\rm min}$ has the same trend, we can confidently say that any ring will arrive at $R_{\rm min}$ earlier than any outside ring to its minimum radius, which, in the latter case, is larger. The physical conclusion is that when the material is moving towards the star, a ring has no interactions with any other ring. The first interaction for material in the orbital plane occurs when a ring arrives at $R = R_{\rm min}$, and begins its journey away from the star. Eventually, this ring will encounter others, forming a shock that will move along with it. Remember that this does not take into account any hydrodynamical effects that will be important when the typical velocities become subsonic. This will happen at some time because the radial velocity eventually will become zero. Pressure forces are expected to change only the location of the minimum radii, as will be shown in § 4, so the block moving outwards is a real feature. A hydrodynamical simulation is our next subject.

4. HYDRODYNAMICAL SIMULATION

4.1. *Description of the code*

For this simulation, we use the hydrodynamical code written by Raga, Navarro-González, & Villagrán-Muñiz (2000), named IGUAZU-A. Fluid equations are numerically solved in a rectangular grid that automatically refines when some criteria are fulfilled. As an example, in a shock, some quantities change rapidly with position, and to resolve this, the code creates the necessary cells.

As the problem we want to address has cylindrical symmetry, the simulation is made in a 2D grid with R and Z as its axes. Assuming that the system is isothermal, the equation of energy is reduced to the statement that the temperature is constant. The code requires an explicit viscosity term. The viscosity coefficient is taken as small as possible so as not to disturb the essential physics of the problem. The assumption of a constant temperature of the disk is not realistic because many processes are expected to occur inside it that can change the temperature profile. In the collapse calculations of Bodenheimer & Laughlin (1995) a disk is found whose temperature ranges between 500 K near the star and 30 K close to the edge, and since the models of D'Alessio, Calvet, & Hartmann (1997) used for the interpretation of the HL Tau spectra require temperatures in that same range, an isothermal assumption for the disk sounds too optimistic. The argument in favor of an isothermal disk for this simulation is that I only want to point out the existence of a mechanism capable of very quickly forming dense structures in the embedded stage, when material is still falling from the cloud. Detailed thermodynamics can change the exact position where material halts its motion towards the star or away from it, but the evolution is dominated by gravitational and centrifugal forces. This be seen in the stationary configuration described in this section, where pressure forces (due to temperature and density gradients) are small compared with either centrifugal or gravitational forces. Clearly, the temperature in the material that falls from the cloud is not relevant because in supersonic motion the information of the density gradients (where the temperature is immersed) cannot communicate particles which are moving so quickly. Thus, a constant temperature throughout the grid can be imposed. Note that this state implies radiation, something that it is always expected.

4.2. *Initial and boundary conditions*

In § 2, we show that Equations (1), (2), (3) and (5) represent a good approximation for the material that is falling towards the star. Thus, we use the velocity field and the density expressed there as initial conditions for the simulation. The terms dependent on $\theta_{\rm o}$ are expressed in terms of r and θ using Equation (4).

To run the code we still have to define the boundary conditions. Two of the sides of the grid are the R-axis and the Z-axis; due to symmetry arguments the perpendicular velocities of the particles are zero. The two other boundaries are defined by $Z = Z_{\rm max}$ and $R = R_{\rm max}$; there, the density and the velocity field are always given by Equations (1),(2), (3) and (5). Physically, this condition means that the material is always fed from the cloud with Ulrich's (1976) solution.

4.3. *Results*

The simulation that we describe now has the following parameters: $R_{\rm d} = 100$ AU, $M = 1\,M_\odot$, $\dot{M} = 10^{-6}\,M_\odot yr^{-1}$, $T = 15\,$K, $\mu = 1.0$ (atomic hydrogen). Avoiding the singularity at the origin, we define a radius ($R_{\rm acr}$) such that the material arriving there is lost from the simulation. The physical dimensions of the axis that defines the computational grid are: $R_{\rm max} = 1000$ AU and $Z_{\rm max} = 100$ AU. Each direction has the same number of cells, that is 512.

When a particular value for $R_{\rm acr}$ is chosen (in this case $R_{\rm acr} = 0.1R_{\rm d}$), the solution of $R_{\rm acr} = R_{\rm min}$ ($R_{\rm min}$ described in equation 14) determines the minimum angular momentum ($\gamma_{\rm min}$) of the material that remains in the plane after the accreting stage (this statement is accurate at any time of the simulation), so, the description of the trajectories since their arrival to the orbital plane and their initial motion towards the star can be described with the ballistic approximation given in § 3. We take Equations (6) to construct a time $t = R_{\rm d}/v_{\rm o}$ (in this case, $t = 158$ yr), which we use as our unit. Using Equation (17), the time of arrival is $t_{\rm min} = 0.197$. Besides, the ring with that particular angular momentum is the first one to arrive to its minimum radius. As mentioned in § 3, with no interactions of the rings when they are moving towards the star, naturally the first interaction occurs when the inner ring changes its direction of motion. In other words, the ring with $\gamma = \gamma_{\rm min}$ produces the first interaction with the material that is still falling onto the orbital plane, at position $R = R_{\rm acr}$. The exact characteristics of the interaction are not easily described.

In Figure 1 we plot, for times less than $t_{\rm min}$, the radial velocity as a function of position. At these times the velocity is always negative, as expected,

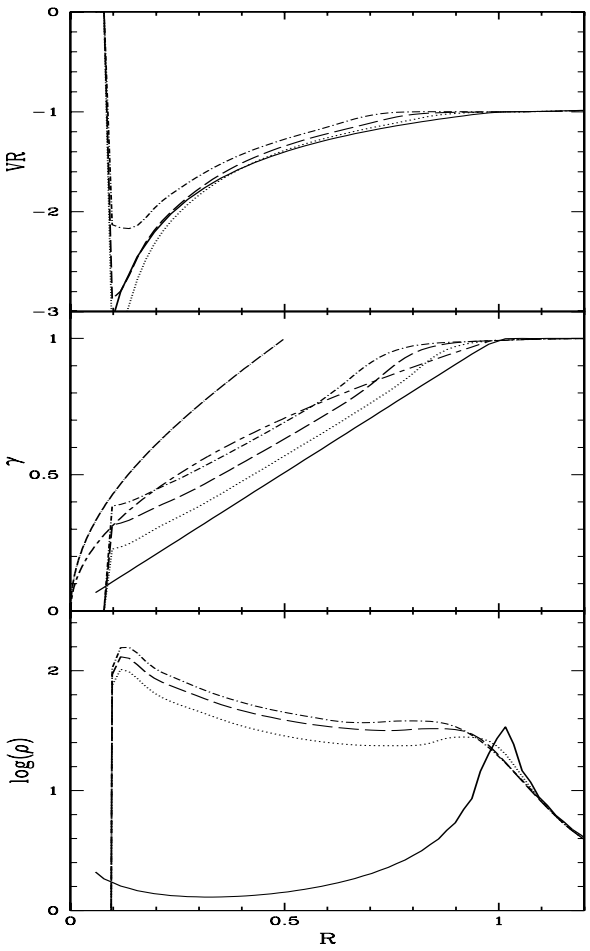

Fig. 1. Hydrodynamical simulation: From top to bottom radial velocity v_R, angular momentum γ and $\log(\text{density}, \rho)$ vs cylindrical radius R in the mid-plane of the disk ($Z = 0$), for times $t = 0$ (solid line), $t = 0.063$ (dotted line), $t = 0.126$ (dashed line), and $t = 0.189$ (dot-dashed line). Also the Keplerian radius ($R_{\rm k}$) is shown as a function of γ ($\gamma = R_{\rm k}^2$) as a dot-long-dashed line. The dot-dashed line represents $R_{\rm min}$. R,v_R, γ and ρ are given in units of $R_{\rm d}$, $v_{\rm o}$, γ_∞ and $\rho_{\rm o}$ respectively (see text).

and we also notice that there is a tendency toward a decrease in magnitude. The above statement is an obvious result of the deceleration process that a particle experiences when approaching $R_{\rm min}$, where $v_R = 0$.

For the same times, we plot in Figure 1 the angular momentum as a function of radius. The important characteristic to describe is that as time increases, the plot is moving towards the origin, nearly preserving its original form, and giving a clear indication of the conservation of angular momentum. Of course, every plot is to the right of the curve of minimum radius, which will be designated as the plot γ vs $R_{\rm min}$ (Equation 14) from now on. This result just corroborates that pressure effects, at most, may change the value of the minimum radius.

Figure 1 also shows the evolution of density in terms of R. From the time $t = t_{\rm min}$ on, a different picture evolves, the ring of material with $\gamma = \gamma_{\rm min}$ will begin to move away from the star. The particles that it encounters will be absorbed into a working surface, accumulating the angular momentum along with the linear momentum. If we assume that the material is perfectly mixed, the ring composed of shocked material will move with the velocity of the center of mass of the components, with a new associated angular momentum, the weighted average of the values of the components.

The evolution of the inner ring is ruled by the material that gets into it from the orbital plane and also from above it. Particles are continually arriving at the plane and interacting with the material that is already in it. The results in § 3 just analyze the particles that initially arrive at the orbital plane without mentioning any further feeding from any other place. At this point of the simulation it is crucial to consider the feeding because the positive velocity of the inner ring creates a void that will interact strongly with material external to the plane, ending with particles that in some way are incorporated into it.

At this moment it is difficult to characterize with precision the material that falls into the void that is forming as a function of time. We can mention two main reasons for that. The first one is that we do not know for sure how the ring evolves in time, and the second is that a well-defined disk is growing in thickness. The thickness is at least an order of magnitude smaller than the radial size of the disk but it is not constant along the radius. The upper boundary of the disk is the surface that divides the accreting material that is not perturbed from the material that already has strong interactions and is no longer represented by the two-body solution (Ulrich 1976). We can characterize precisely the material outside the disk, but to say which particles are incorporated into the disk at some radius demands a clear understandings of its structure.

Let's follow the evolution of the material in the disk for times $t > t_{\rm min}$. In Figure 2, for a time a little longer than $t_{\rm min}$ ($t_{\rm min} = 0.197$), the innermost part of the disk has positive velocities, representing the ring that begins to move away from the star. As time advances, a region opens up with the movement

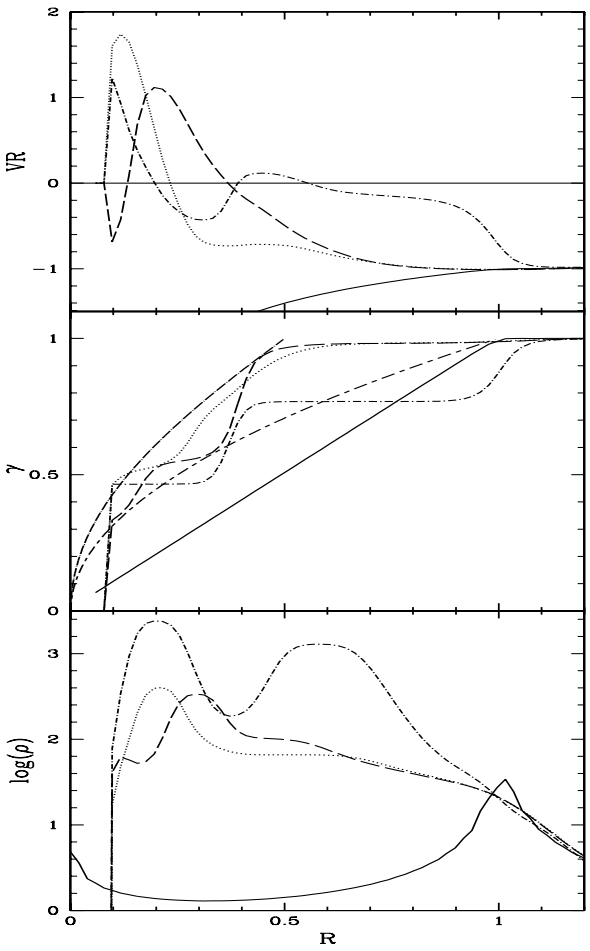

Fig. 2. Similar to Figure 1 but for times $t = 0$ (solid line), $t = 0.442$ (dotted line), $t = 0.569$ (dashed line), and $t = 12.64$ (dot-dashed line). The other curves represent the same as in Figure 1.

of the inner ring and is fed with external material that at some time begins to move towards the star. This configuration clearly divides the ring and the material that is incorporated into it, defined as the pattern with positive velocities, from the particles beside it, that have negative velocities and which represent the material that avoids the ring.

Eventually, material in the innermost part of the disk will move with positive velocities indicating that there exists a point inside the disk where $v_R = 0$. It can be explained as a particular region of the disk which is fed with external material from the inside of it with positive velocity particles, and from the outside of it with negative velocity particles. Looking at Figure 2, where density vs radius is plotted, we directly identify that region as a dense ring that early in the evolution achieves a stationary configuration around the position $R = 0.2R_{\rm d}$. In Figure 2, we also show radius vs angular momentum for $t > t_{\rm min}$. The ring moves from an angular momentum plateau to another with a larger value, indicating that a perfect mix is occurring with the material that incorporates into it, permitting to associate a constant angular momentum to the ring, which increases in time. We can visually identify in a 2D graph (R,Z plane) the statements made before. In Figure 3, at time $t = 0.569$, we can see how the ring moves away from $R_{\rm acr}$ towards regions of steep gradient in angular momentum. Here, the ring is characterized by a maximum in density and constant specific angular momentum.

The information that could be extracted from Figure 3 must be taken with care, in particular in what refers to the thickness of the disk. This feature strongly depends on the details of the heating and cooling mechanisms that are not taken into account here. However, the surface density as a function of radius in the plane of the disk can be compared with real disks.

Figure 2 also shows the stationary configuration to which the system arrives, at a time around $t = 12.64$. The disk consists of two dense rings on Keplerian orbits at positions around $R = 0.2R_{\rm d}$ and $R = 0.6R_{\rm d}$. Between them, a minimum density ring is also at a Keplerian position ($R = 0.4R_{\rm d}$) but it is not characterized by a plateau of angular momentum; instead, it is a region of transition between both plateaus (constant angular momentum).

Returning to the visualization of the system in the R-Z plane for a time $t = 1.264$, Figure 3 shows the next qualitative step in the evolution, where a dense ring, formed with material coming from the cloud, can be seen located inside the ring formed earlier. At this time, all the material that originally falls into the orbital plane had been added to the external ring that is still forming. From now on, the feeding of that ring from the orbital plane proceeds only with material with $\gamma = 1.0$. Particles with less angular momentum come from beyond that plane. The positive velocity pattern is restricted to radius of less than one; it means that the system has not enough lineal momentum to push it beyond radius one. From the results of this simulation it can be concluded that the material accreting in the orbital plane is responsible for stopping the outer dense ring and that other assumptions about the thermal state of the disk may only change the typical size of the structure, but it is very unlikely that the dense structure will not survive.

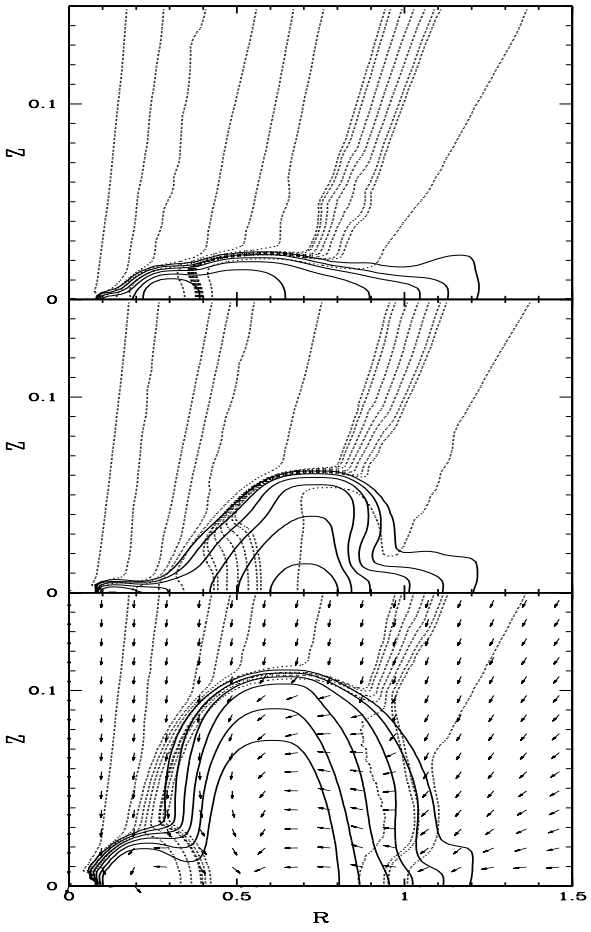

Fig. 3. A RZ plane in the hydrodynamical simulation is shown with contours of equal ρ (solid line) and contours of equal γ (dotted line). The values of the density (ρ) contours are given by $\rho_o/2^a$ (a = 3, 4, 5, 6, 7, 8). The values of the γ contours are: 0.1, 0.2,..., 0.7, 0.71, 0.73, 0.75, 0.77, 0.79, 0.8, 0.9 from left to right. Plots are made at times $t = 0.569$, $t = 1.264$ and $t = 12.64$ from top to bottom. At $t = 12.64$ a stationary configuration is reached. The arrows represent the velocity field, with magnitudes proportional to the size of the arrow.

Figure 3, for $t = 12.64$ (the plot for the stationary situation), shows that the disk is restricted to $R < 1$ as expected, and that the thickness of the external part of the disk is about three times that of the internal one. The contours of constant angular momentum give us an idea about the way the material is incorporated into the disk. In order to extract this information we supposed that by following a specific contour, the trajectory of the particle is also followed. For the last sentence to be true, the flux must be time-independent and the conservation of angular momentum should be valid for every particle, true for stationary fluxes with cylindrical symmetry in the case of unimportant viscous torques.

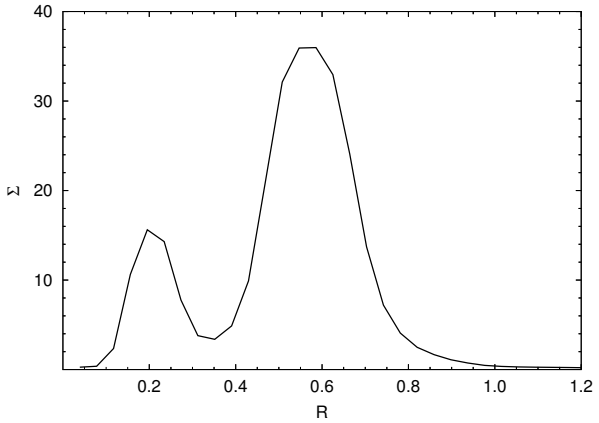

Fig. 4. Surface density S vs radius R is shown for a disk with a mass $M_{\rm d} = 0.02\,M_\odot$. R is given in units of $R_{\rm d}$ and S in g cm^{-2}. This surface density corresponds to an axisymmetric disk viewed pole-on.

Supposing the preceding is true, we can conclude that when the material intersects the disk, the direction of the flow is deflected by a shock, finally sliding along the surface of the disk until it finds its way to the orbital plane. Remembering the form of the disk, the main position where the material is being channeled to the orbital plane is the radius associated with the minimum in density, that is, the region between the two dense rings, as we can see in Figure 3.

In Figure 4 we show the surface density (S) in the disk as a function of radius (R), calculated by vertical integration of the volume density extracted from the hydrodynamical simulation. In this way the thickness of the disk is irrelevant, and we obtain a quantity that can be compared with results of observations of disks. The mass of the simulated disk presented at the bottom of Figure 3 is $M_{\rm d} = 8\,X\,10^{-4}\,M_\odot$. The fact that the disk is in a stationary configuration can be used to scale the mass to any value. Kikuchi, Nakamoto, & Ogochi (2002) find a disk-model with $M_{\rm d} = 0.02\,M_\odot$ for HL Tau, capable of explaining the spectral energy distribution (SED) for the surroundings of this star in a range of frequencies. The scaled simulated disk has densities around 10 g cm^{-2}, as the modeled disk in Kikuchi et al. (2002). Lay, Carlstrom, & Hills (1997), Adams, Emerson, & Fuller (1990), and Kikuchi et al. (2002) use power-law density profiles corresponding to surface densities (S) in the same range as the ones obtained in this work. D'Alessio et al. (1997) show a detailed model for a disk around

HL Tau, which fits the SED for wavelengths from sub-mm to radio. There, an expression for S is found, consistent with a stationary configuration. In the spatial range of interest $S < 100$ g cm^{-2} is also in agreement with the simulated disk shown in this paper. Note that the difference between minimum and maximum densities in Figure 4 is more than an order of magnitude; thus, the pattern should be identified observationally.

The plot in Figure 3 also shows the velocity field, represented by arrows with longitude proportional to the magnitude; so, the rings have been fed with material both from the left and from the right of the center of each ring located at an equilibrium position. Notice that at that point the pressure gradient is zero, because the position corresponds to a maximum in density. Allowing the presence of this hydrodynamical force, a Keplerian radius is still in equilibrium at the center of the ring. Because each ring as a whole is not moving, the addition of lineal momentum from right and left must cancel. Although the condition says something about the kinematics of the incoming material, it cannot disentangle the peculiarities in the velocity of every piece of material with a particular value of the angular momentum. As a matter of fact, the velocities of the particles that are just entering the ring have no direct (analytic) connection with the known solution of Ulrich (1976), therefore we are unable to characterize that material.

4.4. *About initial conditions and changes in the parameters*

For sure, initial conditions can change the outcome of the simulation. However, the relevant gravitational mechanism forming the pattern with two rings in the disk dominates initial conditions, since a lower-mass disk has already formed. One way to face the problem is to think that a stationary configuration, as the one found here, can act as a initial configuration that would naturally preserve the features of the disk. However, this configuration will not last, because after a certain time the disk will have accumulated enough mass, arriving at a configuration prone to gravitational instabilities. After the action of the instability, the disk will achieve a stable state that, as a first guess, can be described with a power-law density profile.

Thus, a natural initial condition (other than no-disk) to test in a simulation is a disk with a surface density of the form $S = S_0 R^{-3/2}$, where the constant S_0 is fixed by the choice of the mass of the disk. The chosen exponent is selected according to Kikuchi et al. (2002) who used it to fit the flat-spectrum of T Tauri stars. Besides, the fitting of HL Tau by Lay et al. (1997) also requires an exponent of less than minus one. As a matter of fact, changing the exponent does not change appreciably the typical densities in the disk; therefore, this simulation attempts to be characteristic. The initial velocity field is Keplerian. The disk is thin, with a thickness of $\Delta Z = 1\,AU$; the mass of the disk is $M_d = 0.01\,M_\odot$. The simulation was followed until a time $t = 9.48$. It is shown in Figure 5 for the radial velocity (V_R), specific angular momentum (γ) and density(ρ) on the orbital plane, in terms of radius (R). The times shown are $t = 3.16, 6.32, 9.48$.

The simulation was run for a time sufficient to allow to look for trends. The density of the initial disk is larger than the typical density in the cloud. Thus, a strong discontinuity in the boundary between disk and cloud is responsible for a transient in the simulation, not seen in the main simulation. At the top of Figure 5, the feature of positive radial velocity close to the star can be seen at the three times, analogous to the same plot in Figure 2. At $t = 9.48$, there are three positions where $V_R = 0$, corresponding to places where the inner and outer rings are fed. At the bottom of Figure 5 the presence of the former becomes obvious, while the latter is in the process of formation. The middle plot in Figure 5 clearly shows that the dense rings sit at a Keplerian radius according to their specific angular momentum. As a conclusion, a not very massive disk initially seeded shows no qualitative changes to the picture already formed, as shown in Figure 5.

The problem depends on dimensionless parameters; in this case, size of the disk, mass of the star, angular velocity of the cloud and mass accretion rate of the cloud into the star-disk system are variables that can be given any value; the results are just scaled to the new configuration. However, there is another variable that should be treated separately, that is $R_{\rm acr}$, the radial size of the inner region of the mesh, where the material is lost.

For computational convenience, a specific value for $R_{\rm acr}$ was chosen to remove material from the center of the disk. As stressed in § 3, $R_{\rm acr}$ allows us to estimate the specific angular momentum of the innermost material that turns around in the early evolution of the particles in the disk. Afterwards this material will become the outer ring, and the material that falls from the cloud with values of specific angular momentum around this value will eventually form the inner ring. As noted, the general features of this process do not depend on the value of $R_{\rm acr}$; thus, the

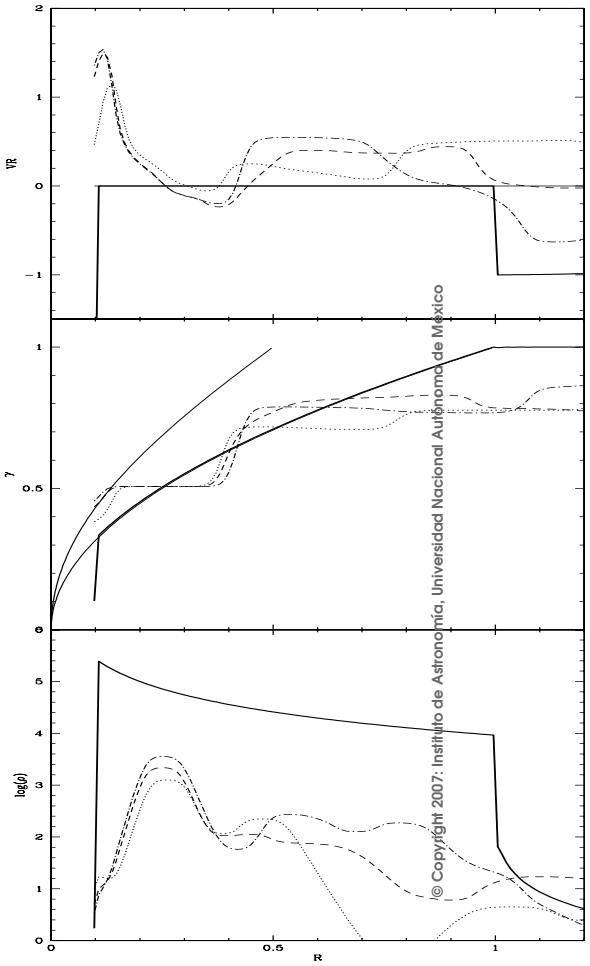

Fig. 5. Similar to Figure 1, but for times $t = 0$ (solid line), $t = 3.16$ (dotted line), $t = 6.32$ (dashed line),and $t = 9.48$ (dot-dashed line). The other curves represent the same as in Figure 1. A Keplerian disk with power density profile is given as an initial condition. The thickness of the disk is $\Delta Z = 1\,AU$ and the mass of the disk is $M_d = 0.01\,M_\odot$.

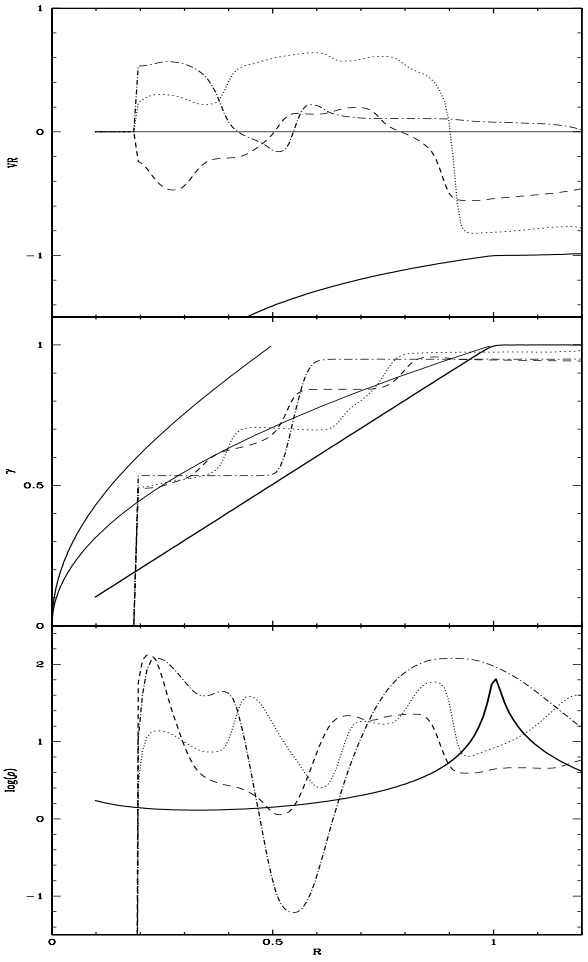

Fig. 6. Similar to Figure 1, but for times $t = 0$ (solid line), $t = 3.16$ (dotted line), $t = 6.32$ (dashed line), and $t = 25.28$ (dot-dashed line). The other curves represent the same as in Figure 1. The difference with the simulation presented in Figure 1 is that $R_{\rm acr} = 0.2\,R_d$ instead of $R_{\rm acr} = 0.1\,R_d$.

two-dense-rings-pattern disk will form, with the only difference that the rings will be located at different positions.

In order to check this theoretical statements, a simulation with $R_{\rm acr} = 0.2\,R_d$ was run (twice the value used). Figure 6 shows V_R,γ and ρ vs R, in the middle of the disk, for $t = 3.16, 6.32, 25.28$. At the first two times, the transition towards the configuration shown at the last time, $t = 25.28$ is shown. The radial velocity plot in Figure 6 shows the same features as in the stationary configuration of Figure 2. The density profile clearly shows the two dense rings, which as expected, are shifted to larger radii, because the average γ in the disk is larger than the one in the case with $R_{\rm acr} = 0.1R_d$. The middle plot in Figure 6 again shows that the specific angular momentum of the rings is constant and that they sit on Keplerian radii.

This result proves that $R_{\rm acr}$ is irrelevant for the formation of the pattern in the disk, changing only the equilibrium positions of the rings.

5. DISCUSSION

As mentioned in the introduction and pointed out by many authors (Bodenheimer & Laughlin 1995; Yorke & Bodenheimer 1999; Nakamoto & Nakagawa 1994; Boss 1998), the formation of gravitational instabilities in a disk is present at the early stages of

the formation of planets. Thus, the axisymmetric configuration obtained in the simulation of § 4 will be subjected to perturbations that can break the rings. The two-dense-rings pattern forms naturally, considering a continuous accretion from the cloud. The outer ring is constructed by sweeping the original matter in the orbital plane, and reaches an equilibrium configuration due to all the material that is still falling from the cloud.

The inner ring is composed mostly of particles with angular momentum around $\gamma_{\rm min}$, and is almost completely fed with material that comes from above the orbital plane. As the details of its formation are complex, we decided not to follow further this path.

The hydrodynamical simulation (see § 4) avoids the identification of a precise radius where the outer ring stops, but surely it is less than, but close to, one.

By now, a qualitative picture can be extracted from the way the material in the orbital plane is being incorporated into the ring at the first stage, finding a stationary position later on, when continuous feeding of the cloud is assumed (see § 4). In summary, the aim of this paper is just to point out that there exists a robust mechanism for forming dense structures during the stage when material is falling into the disk from the cloud. We leave a study of a realistic thermic scheme for the future.

6. CONCLUSIONS

The collapse of a core (observational characteristics of the cloud in Jijina, Myers, & Adams 1999) is studied with the purpose of describing the formation and early evolution of a disk. We examine a situation where a central mass exists inside the cloud, and is responsible for the main force that the particle experiences. Neglecting self-gravity and pressure is a valid assumption if we consider a disk much less massive than the central object, with typical supersonic velocities. All these assumptions are naturally taken into account in the collapse solution of Ulrich (1976). So, in § 4 this solution is used as an initial condition for an axisymmetric hydrodynamical simulation. The material falls to the orbital plane with the subsequent formation of a disk, by way of two shocks, one at the top of the disk and the other at the bottom. Afterwards, all the material moves towards the star until the inner part of the disk (we call it the inner ring) begins to move in the opposite direction. This ring begins to sweep material that is still accreting towards the central mass, finally finding an equilibrium position at a Keplerian radius ($R_{\rm k} = 0.6$, see Figure 3).

The matter incorporated into this dense ring mixes perfectly, imparting to it its linear and angular momentum. The first quantity is a contribution to the velocity of the shocked ring and the last one allows to associate to the ring just one value of its specific angular momentum. From this value we can assign a Keplerian radius to this ring.

The positive velocity stage of the ring creates a region inside it, fed with material that is still falling from the cloud. These particles have restricted possibilities for the specific angular momentum, with values close to $\gamma_{\rm min}$ (see § 3). Early in the evolution this material evolves to form a dense ring with constant specific angular momentum that sits at the appropriate Keplerian radius ($R_{\rm k} = 0.2$, see Figure 3).

Formation of rings (Tohline 1980; Pickett et al. 2003; Boss 1980; Larson 1972; Black & Bodenheimer 1976; Bodenheimer & Tscharnuter 1979) is an important outcome if we are interested in mechanisms forming denser zones in disks as progenitors of planets or companion stars. But the question we always ask is the life-time of the feature (Boss 1980), since its viability for forming a stable structure such as a planet depends on it. Thus, in Nagel (2007) we use the isothermal spherically symmetric collapse model of Shu (1977), and obtain a similarity solution in terms of the disk radius at any time (as a first order approximation), as well as a typical value for the time required for the collapse, at least a couple of orders of magnitude larger than the time for the formation of the stationary two-dense-rings-pattern disk; so, a quasi-stationary picture can easily be considered, where a stationary disk will continuously evolve from one configuration to another. However, this configuration naturally produces rings that are continually increasing in mass, and so, at some point, gravitational instabilities will break up the rings, giving rise to the formation of a set of dense regions that will leave an imprint on later stages, with zones prone to planet formation. All the arguments used in this explanation require the material to continue falling from the cloud. So, if the cloud is exhausted, the survival of the two-dense-rings-pattern disk for longer times is not clear, thus reducing the possibilities of observation. To clarify this doubt, we use the simulation of § 4 and after the formation of the pattern, we reduce the density of the falling material by a factor of 10 in order to simulate the exhaustion of the cloud. We see that after 40000 yr, the dense rings are still there, but located at different positions, still within $R < 1.0$. Therefore, in some cases, this feature can be observed if we can detect a disk

deeply embedded in its parental cloud. As a matter of fact, Piétu et al. (2005) found a bright, spiral-like feature at about 140AU from AB Auriga that could be produced in an early stage of star formation.

Using a typical value for the time required for the formation of the two-dense-rings pattern (§ 4) we can argue that the positions of the two rings and the radius of the disk expand as t^3. In Stahler et al. (1994) a similar structure, but with just one ring, expands in the same way. The position of the ring in Stahler et al. (1994) ($R = 0.345$) is closer to the minimum density on the orbital plane that coincides with the boundary between the two dense rings, as shown by the simulations of § 4. The conjecture about the reason for the nonexistence of the two rings (that we found here) in Stahler et al. (1994) is that there the formation of the ring is linked to the assumption that the material at the left of this ring strongly dissipates energy inside a turbulent layer, before coming finally to a Keplerian orbit. What we say here is that the streamlines of the "outer disk" (see details in Stahler et al. 1994) intersect at the position of the ring, making it unable to change the sense of its movement to face this established part of the disk. This means that the outer ring in Figure 3 is represented by the ring in Stahler et al. (1994). According to the construction, an inner ring in the "inner disk" (the Keplerian part of the disk) in Stahler et al. (1994) cannot exist.

The main idea for the formation of the ring in the simulation of § 4 is that at some point the material in the disk is halted, so afterwards a positive net force dominates (here, the centrifugal dominates over the gravitational), driving this ring to a larger radius. Arguments like this for explaining the ring formation are not new (Tohline 1980; Boss 1980; Larson 1972; Black & Bodenheimer 1976; Bodenheimer & Tscharnuter 1979), but the purpose there was only to study this formation in cloud collapse without any central mass. In the simulations (Tohline 1980; Boss 1980; Larson 1972; Black & Bodenheimer 1976; Bodenheimer & Tscharnuter 1979) the gravitational potential comes from self-gravity; in our work the gravitational contribution comes only from the proto-star, although the ideas used for explaining the ring formation are the same in both cases.

Returning to the outer ring formation, the simple idea that we follow is that the first material that turns around to begin a positive velocity evolution is the seed of the ring that evolves outwards. The simulation shows the ring at radius of less than one; essentially, this fact means that these dense features are restricted to a smaller radius than the radius of the disk, defined as the position of the larger Keplerian orbit.

The radial velocities in the stationary configuration are small as compared with the angular velocities in a Keplerian disk; so, a kinematic observation of the disk can easily overlook the small radial velocities to conclude that the observed disk is Keplerian. Therefore, we hope that this result can motivate an effort to estimate radial velocities in disks, to be compared with the state found here. Such a pattern in the disk has more chances to exist in sources deeply embedded in a cloud, where observations are more difficult. However, recent results (Velusamy, Langer, & Goldsmith 2002) show methanol emission tracing an infall-disk interface; so we expect that future observations can constrain embedded disks. An observational consequence of the disk here described occurs if the dense rings are optically thick while the remaining of the disk is optically thin. In such a situation the emission of radiation should be dominated by the rings, producing a peculiar energy spectrum with certain preferred frequencies.

I thank J. Cantó and A. Raga for their continued support and advice. The assistance of A. Raga in the numerical part of this research is gratefully acknowledged. I also thank J. Cantó for a critical reading of the original version of the paper.

REFERENCES

Adams, F. C., Emerson, J. P., & Fuller, G. A. 1990, ApJ, 357, 606
Bate, M. R. 2000, MNRAS, 314, 33
Black, D. C., & Bodenheimer, P. 1976, ApJ, 206, 138
Bodenheimer, P., & Laughlin, G. 1995, RevMexAA (SC), 1, 157
Bodenheimer, P., & Tscharnuter, W. 1979, A&A, 74, 288
Boss, A. P. 1980, ApJ, 237, 563
_____. 1998, ApJ, 503, 923
Cassen, P., & Moosman, A. 1981, Icarus, 48, 353
D'Alessio, P., Calvet, N., & Hartmann, L. 1997, ApJ, 474, 397
Hayashi, M., Ohashi, N., & Miyama, S. M. 1993, ApJ, 418, L71
Hueso, R., & Guillot, T. 2002, BAAS, 34, 888
_____. 2005, A&A, 442, 703
Hunter, C. 1963, MNRAS, 126, 299
Jijina, J., Myers, P. C., & Adams, F. C. 1999, ApJS, 125, 161
Kikuchi, N., Nakamoto, T., & Ogochi, K. 2002, PASJ, 54, 589
Larson, R. B. 1972, MNRAS, 156, 437

Laughlin, G., & Bodenheimer, P. 1994, ApJ, 436, 335
Lay, O. P., Carlstrom, J. E., & Hills, R. E. 1997, ApJ, 489, 917
Lin, D. N. C., & Pringle, J. E. 1990, ApJ, 358, 515
Lynden-Bell, D., & Pringle, J. E. 1974, MNRAS, 168, 603
Mundy, L. G., Looney, L. W., & Welch, W. J. 2000, in Protostars and Planets IV, ed. V. Mannings, A. Boss, & S. Russell (Tucson: Univ. of Arizona Press), 355
Nagel, E. 2007, PhD Thesis, Universidad Nacional Autónoma de México
Nakamoto, T., & Nakagawa, Y. 1994, ApJ, 421, 64
Padgett, D. L., Stapelfeldt, K. R., & Sargent, A. F. 2000, BAAS, 32, 1481
Pickett, B. K., Mejía, A. C., & Durisen, R. H. 2003, ApJ, 590, 1060
Piétu, V., Guilloteau, S., & Dutrey, A. 2005, A&A, 443, 945
Raga, A., Navarro-González, R., & Villagrán-Muniz, M. 2000, RevMexAA, 36, 67
Shu, F. H. 1977, ApJ, 214, 488
Shu, F. H., Adams, F. C., & Lizano, S. 1987, ARA&A, 25, 23
Shu, F. H., Najita, J., & Ostriker, E. 1994, ApJ, 429, 781
Stahler, S. W., Korycansky, D. G., Brothers, M. J., & Touma, J. 1994, ApJ, 431, 341
Strom, S. E., Edwards, S., & Skrutskie, M. F. 1993, in Protostars and Planets III, ed. E. H. Levy & J. I. Lunine (Tucson: Univ. of Arizona Press), 837
Terebey, S., Shu, F. H., & Cassen, P. 1984, ApJ, 286, 529
Tohline, J. E. 1980, ApJ, 236, 160
Tscharnuter, W. M., & Boss, A. P. 1993, in Protostars and Planets III, ed. E. H. Levy & J. I. Lunine (Tucson: Univ. of Arizona Press), 921
Ulrich, R. K. 1976, ApJ, 210, 377
Velusamy, T., Langer, W. D., & Goldsmith, P. F. 2002, ApJ, 565, L43
Yorke, H. W., & Bodenheimer, P. 1999, ApJ, 525, 330

E. Nagel: Instituto de Astronomía, Universidad Nacional Autónoma de México, Apdo. Postal 70-264, 04510 México, D. F., México (enagel@astroscu.unam.mx).